

Deep Profiling of Agroecological Resilience based on Self-Organized Productivity

Masatoshi Funabashi (✉ masa_funabashi@csl.sony.co.jp)

Sony Computer Science Laboratories, Inc.

Article

Keywords: Primary Food Production, Biodiversity Loss, Low-input Mixed Polyculture, Synecoculture

Posted Date: January 3rd, 2024

DOI: <https://doi.org/10.21203/rs.3.rs-80005/v2>

License:  This work is licensed under a Creative Commons Attribution 4.0 International License.

[Read Full License](#)

Additional Declarations: The authors declare no competing interests.

1 **Title: Deep Profiling of Agroecological Resilience based on Self-Organized**
2 **Productivity**

3
4 **Author**

5
6 **Masatoshi Funabashi^{1,2}**

7 1. Sony Computer Science Laboratories, Inc. Tokyo, Japan

8 2. Research Division on Social Common Capital and the Future,

9 Kyoto University Institute for the Future of Human Society, Kyoto, Japan

10 **e-mail:** masa_funabashi@csl.sony.co.jp

11
12
13 **Article summary**

14 Transformative change in primary food production is urgently needed in the face of
15 climate change and biodiversity loss. Although there are a growing number of studies
16 aimed at global policymaking, actual implementations require on-site analyses of
17 social feasibility anchored by ecological rationale. This article reports the in-depth
18 characterizations of low-input mixed polyculture of highly diverse crops managed on
19 the self-organization of ecosystems, which performed better compared to
20 conventional monoculture methods in Japan and Burkina Faso. Analyses on crop
21 productivity and diversity showed that the primary production of ecosystems followed
22 a power law, and through the underlying mechanisms excelled in 1) promoting
23 diversity and total quantity of products along with the rapid increase of in-field
24 biodiversity, especially useful for the recovery of local regime shift in a semi-arid
25 environment; 2) a fundamental reduction of inputs and environmental load; and 3)
26 ecosystem-based autonomous adaptation of the crop portfolio to climatic variability.
27 The overall benefits imply substantial possibilities of a new typology of sustainable
28 farming for smallholders sensitive to climate change, which could overcome the
29 historical trade-off between productivity and biodiversity based on the human-guided
30 augmentation of ecosystems.

31
32
33
34 **Introduction**

35
36 Many studies have sounded alerts about global ecological deterioration due to the
37 accelerating impacts of human activity in the last century (e.g., ref. 1-4). The 6th
38 mass extinction is considered underway in a wide range of biotic communities,
39 including primary forests⁵, vertebrates⁶, and insect fauna⁷.

40 These impacts are largely due to the primary food production on land and have
41 caused critical environmental shifts in marine ecosystems⁸: Here, the agricultural
42 sector is responsible for 25% of greenhouse gases (GHGs)⁹, and it has disrupted global
43 biochemical flows and biosphere integrity¹⁰. However, interactive responses to
44 changes in human activities, material cycles, and biodiversity distribution, including
45 effects induced by climate change mitigation and conservation activities, are extremely
46 complex and difficult to simulate. Globally assessed scenarios (e.g., ref. 4, 11) are not
47 capable of predicting actual social emergencies, such as the COVID-19 pandemic, and
48 cannot promptly address the root causes. Moreover, the importance of an integrated

49 approach to the science of climate and biodiversity changes and the development of
50 coherent policies has only recently been realized (e.g., ref. 12). Current economic
51 theory and practice do not sufficiently incorporate a valuation of biodiversity and
52 multiple ecosystem services¹³; we need to take comprehensive measures
53 interconnecting direct drivers of ecosystem deterioration and underlying economic,
54 social, and technological causes, in order to regenerate the ecologically driven material
55 cycles and substantially reducing agricultural inputs and runoff^{3,14}.

56 Many global-scale simulations have suggested possible scenarios
57 toward sustainable land use aimed at recovery of biodiversity and the carbon
58 cycle (e.g. ref. 15, 16). On the other hand, despite their scale, these studies are
59 based on databases that do not necessarily encompass the whole social-
60 ecological complexity required for an actual implementation. The interactions
61 of many parameters and the complexity of community dynamics have largely
62 been ignored (e.g., in a food-system change scenario¹⁵, the cross-field
63 phosphorus cycle¹⁷ and management breakthrough on the carbon cycle¹⁸ are
64 not included; in a global afforestation scenario¹⁶, the implausibility of
65 afforestation of naturally maintained grasslands and savannas and
66 thermodynamic trade-off between tree cover increase and consequent
67 diminishment of albedo¹⁹ are not considered), and deep case studies are
68 needed in connection to a realistic driving force. The ground truth is often
69 ignored even in basic statistical studies; this makes the applicability of global
70 scenarios to actual situations quite elusive— while 84% of some 570 million
71 farms are owned by smallholders producing on less than 2 ha, estimates of the
72 total surface of smallholds vary from 12% to 40% of the global farmland
73 depending on the method of measurement²⁰.

74 Through recent meta-analysis, significant research gaps are identified²¹
75 in 1) how to double the incomes and productivity of small-scale food
76 producers; 2) how to make food production more environmentally sound and
77 more resilient to climate shocks and other disasters; and 3) how to respond the
78 needs of smallholders and their families within local contexts with the support
79 of original data.

80 In order to convert the majority of food producers, especially resource-,
81 knowledge-, and technology-deprived smallholders into positive drivers of
82 biodiversity, on-site tailoring and proactive management of agrobiodiversity in a
83 comprehensive social-ecological context are important leverage points^{3,22}. An essential
84 pillar of transformative change in food production is to deliver a management-
85 intensive typology of sustainable practices that contains interfaces with the diversity
86 and uniqueness of real-world operations on a scientific basis, which has been studied
87 in the field of open complex systems science^{14,23,24}. We need complementarity between
88 a general theory based on averaged statistics and deep analyses of significant
89 individual cases in order to make progress toward the inclusion of neglected diversity.
90 With the rise of big data, such a paradigm has emerged in the management of living
91 systems, such as in precision medicine (e.g., N-of-1 studies²⁵ and other longitudinal
92 deep phenotyping), yet to be applied for Planetary Health, which is a solution-oriented
93 interdisciplinary field and social movement on the well-being of all living organisms
94 through analyzing and addressing the impacts of human disruption to the Earth's
95 natural systems²⁶. This study aims to provide the agroecological rationale for such a
96 novel paradigm through elaborate characterizations of pioneering cases that are

97 compatible with the application to the grass-root majority of world food production.
98
99

100 **Results**

101 **Crop production at ecological optimum**

102 Empirical studies in ecology have revealed the positive contribution of species
103 diversity and the symbiotic relationship between plants to the primary production of
104 ecosystems at the community level (e.g., ref. 27), especially in relation with surface
105 patterns that follow power-law distribution^{28, 29}. Although knowledge of self-
106 organized natural vegetation constitutes a better understanding of community
107 dynamics and has been used for planning conservation practices, little of it has been
108 applied to crop production.

109 Synecological farming (synecoculture) takes advantage of the sustainable
110 productivity of self-organized vegetation that occurs when there is an extremely high
111 diversity of crops^{14,30,31}. The principle of production in synecoculture is fundamentally
112 different from those of other low-input organic and natural farming methods that are
113 limited in their association and rotation of a few crops (e.g., ref. 32). In contrast to the
114 conventional definition of productivity based on a single crop and a field environment
115 controlled toward its physiological optimum, synecoculture relies on the primary
116 production of a mixed community that comprises tens to hundreds of edible plant
117 species; this sort of production is known as augmentation of the ecological optimum
118 (explained in Box 1).

119

120 **Symbiosis-dominant ecosystems with crops**

121 To evaluate the self-organization process of a mixed community of crops, we chose a
122 practice on a 420-sq.m plot in the temperate zone (Oiso, Japan) to measure the species-
123 wise surface at the early stage of synecoculture introduction (Fig 2 (a1-a4): field A).
124 The inverse cumulative distribution of the species diversity on the surface was closer
125 to a power-law distribution than an exponential distribution, implying that the
126 symbiotic interactions between plants are inherent besides the competition for
127 resources (Fig 3 (a), see Methods).

128 The probability density of the species-wise surface in each 2-sq.m
129 measurement section also followed a power law (Figure 5 (top) of the Extended Data).
130 The relative degree of symbiotic relationship can be compared with the parameter λ
131 and showed that naturally occurring spontaneous species (usually considered to be
132 weeds) form vegetation patterns that contain more positive interactions (λ closer to
133 zero) than the introduced crop species. This tendency was also observed in another
134 classification of edible and non-edible plants based on past usage in synecoculture
135 practices. Positive diversity responses to climate variability were also dominant in
136 spontaneous species (see Fig 2 of Extended Data). The direct implication is that the
137 coexistence of naturally occurring non-edible species serves as a substantial source of
138 symbiotic gain for the whole community dynamics that promotes ecological
139 succession, and it may contribute to the productivity of crops and other edible plants
140 through an overall increase in resources such as soil organic matter and soil microbial
141 activity³³.

142

143 **Production experiments**

144 The productivity of synecoculture in temperate and semi-arid tropical zones was
145 tested in two farms, on a 1,000 sq.m farm in Ise, Japan over the course of four years
146 (Fig 2 (b1-b2): field B) and on a 500 sq.m farm in Mahadaga, Burkina Faso over the
147 course of three years (Fig 2 (c1-c5): field C). The probability density of product-
148 sales data based on asynchronous thinning of highly diverse mixed polyculture
149 showed a long-tail distribution that largely deviated from a conventional normal
150 distribution (Fig 4 (a, b) and Fig 5 (a,b)), and it followed power law (See Figure 5
151 (middle and bottom) of the Extended Data, and examples of harvests in Fig 2 (b2) of
152 the main text), regardless of the differences in climate region and species
153 composition.

154 Despite the no-input practice except water and introduction of seeds and
155 seedlings, on-site observation implied overall and multiple increases in ecosystem
156 functions along with the ecological succession in the fields, such as improvement in
157 crop yield, the establishment of a complex food chain that supported ecological
158 regulation of pests, thick development of porous soil structure, increased humus and
159 soil organic matter, improved water retention and permeability, and the resulting
160 activation of soil microbiota (see e.g., Fig 2 (c4-c5), Figure 6 (a1) and (b1) of the
161 Extended Data, and ref. 24, 30, 34).

162 The average profitability (measured as gross sales minus costs) of
163 synecoculture in the field B rose 2.35- to 3.87-fold, which corresponds to an estimated
164 0.981- to 1.16-fold increase in harvest biomass, compared with the conventional
165 databases of all scales and small scale (<0.5ha) (see the description of the relative
166 biomass ratio BR in Methods). Compared with the median (and 25th and 75th
167 percentiles) of conventional market gardening, the profitability of synecoculture in the
168 field C rose 88.0(202/54.4)-fold, which corresponds to an estimated 33.8(49.6/25.1)-
169 fold increase in harvest biomass, on average over two 18-month periods before and
170 after November 2016 under different social conditions. In particular 121(278/74.9)-
171 fold increase in profitability corresponding to an estimated 37.8(55.3/28.0)-fold
172 increase in harvest biomass under high market accessibility, and a 55.0(126/34.0)-fold
173 increase in profitability corresponding to a 29.9(43.8/22.2)-fold increase in harvest
174 biomass under low market accessibility (see Methods). The on-site comparison at the
175 field C showed that synecoculture excelled in showing 258-fold increase profitability
176 in correspondence with an estimated 12.4-fold harvest biomass compared with the five
177 other simultaneously tested alternative methods of sustainable farming.

178 A most dramatic change was the local reversal of the regime shift in the field
179 C. From an analysis of satellite images taken before the experiment, the vegetation
180 patches that surrounded the field C corresponded to spotted vegetation patterns that
181 strongly implied warning signals of imminent desertification³⁵. The subsequent
182 intensive introduction of 150 edible plant species, including 40 staples, reestablished a
183 lush ecosystem that maintained high productivity year-round that had positive
184 regeneration effects on neighboring plots (Fig 2 (c1-c3)). The established ecosystem
185 comprised typical plant types that reach to a mature vegetation succession stage, such
186 as pioneering annual and perennial plants, shrubs and vines, light-demanding trees
187 and shade-tolerant trees.

188

189 **Climate resilience**

190 In all of the experiments conducted at the three sites, a significant positive correlation
191 of plant species diversity with the fluctuation components of major meteorological
192 parameters was observed, which could not be totally reduced to a correlation with the
193 mean components (Fig 3 (b), Fig 4 (c), and Fig 5 (c) of the main text and Figs 2-4 of
194 the Extended Data). The observed biodiversity response can be considered as an
195 adaptive diversification of the species composition to climatic variability³¹ rather than
196 seasonal patterns in community dynamics, because seasonality was weaker in the
197 fluctuation than in the mean components due to the non-linear relationships between
198 the mean and standard deviation of meteorological parameters (bottom line of Figs 2-4
199 of the Extended Data). The observed positive correlation between the meteorological
200 variance and plant species diversity in self-organized edible ecosystems implies the
201 presence of evolutionary acquired biodiversity maintenance mechanisms, because
202 increasing diversity to cope with environmental fluctuation generally contributes to
203 sustain ecological community. Such community-level responses could constitute a
204 fundamental mechanism to augment the climate resilience by mainstreaming
205 biodiversity in food production³⁶, which could provide an enhanced portfolio of
206 agrobiodiversity beyond substitution and relocation of major crops³⁷, and thereby
207 enlarge the range of options to cope with the ineluctable global biodiversity
208 redistribution under climate change³⁸ and keep the food systems within the planetary
209 limits^{15,39}.

210
211

212 **Discussion**

213

214 One of the greatest challenges in this study that seems contradictory to conventional
215 monoculture methods is the stabilization of yield that relies on ecological niche
216 formation. The rationale of synecoculture lies in productivity at the community level
217 with an extensive portfolio of products and reduced input costs, which is compatible
218 with the primary production of self-organized plant communities in natural
219 environment³⁰. In Figure 5 of the Extended Data, although the fitted Pareto
220 distributions for all experiments are situated in the parameter range where analytical
221 mean converges to a finite value (i.e., $a > 1$), a large deviation is inherent even at the
222 annual scale (the 12-month gross sales ranged between 56 and 141% of the total
223 average for the field C and was between 27 and 214% of the total average for the field
224 B). Therefore, productivity in terms of arithmetic means is not a stable indicator for
225 management. Still, the cumulative cost-benefit ratio converged to a higher level of
226 performance compared with the conventional and other alternative methods (Figure 6
227 (a2) and (b2) of the Extended Data), which conforms to the theoretical prediction of
228 power-law productivity and stability of harmonic means in our previous study³¹. This
229 is due to the positive correlation of productivity with introduced species diversity that
230 develops over time, which is particularly enhanced in the ecological optimum
231 production and performs increasingly better in marginal environments for both gains in
232 gross sales and cost reductions (see total overyielding in Fig 1 of the main text and
233 Figure 1 of Extended Data for the theoretical predictions, and Figure 6 (a1) and (b1) of
234 the Extended Data for the measured data).

235

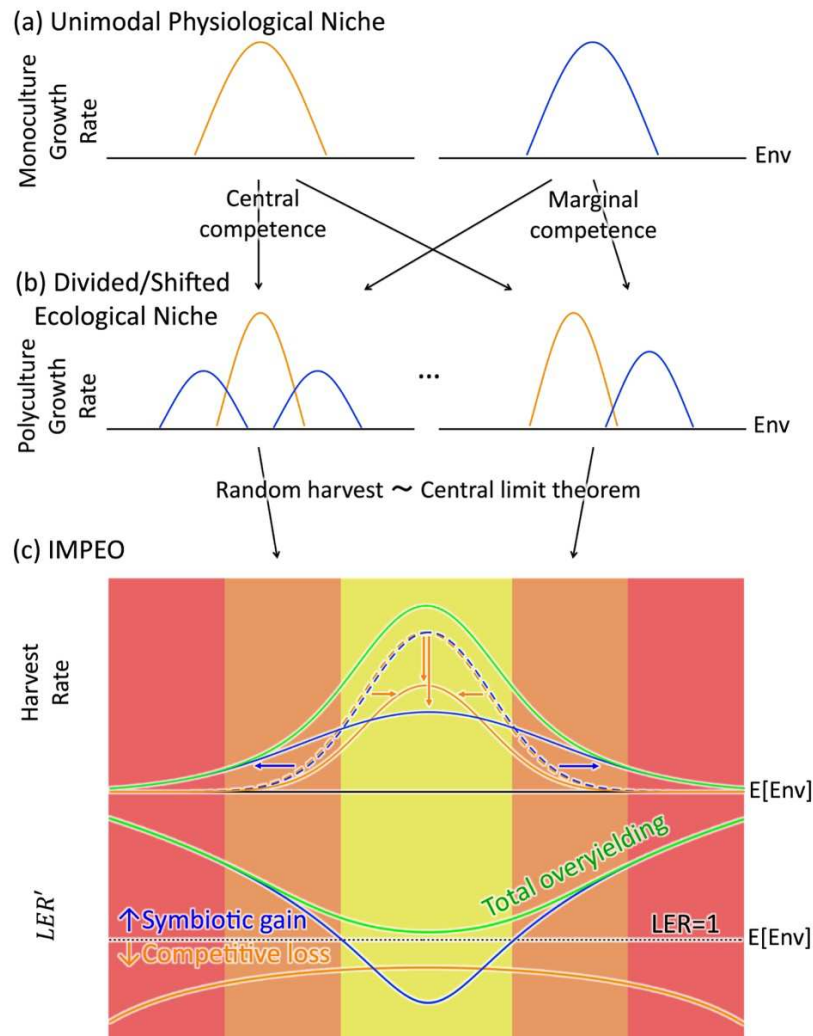
Not only the higher productivity of the field C, but also the ecological

236 optimization with synecoculture could rebuild the power-law distribution of patch
237 patterns and may help to prevent state shifts in the farm plots near the living area in a
238 semi-arid environment^{35,40}. The recovery and enhancement of diverse vegetation in
239 farm plot represents a major shift from negative to positive externality on biodiversity
240 in crop production¹⁴, which is also compatible with massive greening initiatives to
241 reestablish a viable environment against desertification (e.g., ref. 41). It also sets a
242 new baseline of increased crop diversity and yield against the declining trend in
243 dryland¹¹, which can minimize land clearing and protect habitats of threatened large
244 mammals especially in sub-Saharan Africa⁴², where animal-source foods are
245 nutritionally valuable in food-deficient settings⁴³. Given the importance of
246 sustainability of smallhold farms and the positive social-ecological impacts that
247 synecoculture could have, international initiatives in ECOWAS are being formed to
248 better utilize the capacity of ecological optimum production, with a short-term goal to
249 provide healthy and balanced diets to 3.5 million people impacted by COVID-19⁴⁴.

250 Asia and sub-Saharan Africa will see the largest growth of agricultural
251 emissions and will account for two-thirds of the increase in overall food demand by
252 2050⁴⁵. In the face of climate change and current pandemics, food systems that support
253 these regions and other nations harboring smallholders need to be scaled bottom up
254 and should realize synergy between provisioning and regulating services (including
255 pathogen suppression) that have been historically put in massive trade-off in
256 agricultural land use^{1,3}. In accordance with the biodiversity maintenance mechanisms
257 that have been progressively revealed in the field of community ecology, our in-depth
258 operational case studies imply that there exist fundamental principles that bring about
259 such synergy through the leveraging of self-organized edible plant communities. It
260 will lead to a novel typology for transformative change from resource- to
261 management-intensive farming capable of creating essential biodiversity and
262 ecosystem services in highly resilient form without resorting to fertilizers and
263 agrochemicals. The diversity-driven productivity reported in this study has a potential
264 to greatly improve improper agricultural practices, especially in the semi-arid
265 environment, which coincides with a part of necessary conditions to upwardly recover
266 the biodiversity decline in many global scenarios. With appropriate development of
267 supportive information technologies^{24,46} and sustainable distribution networks for
268 various farm products⁴⁷ and neglected and underutilized plant genetic resources⁴⁸,
269 ecological optimum production could be applicable to small-scale farms less than 5 ha
270 that make up 94% of agricultural holdings⁴⁹ and which combined with middle-scale
271 farms less than 50 ha produce up to 77% of the major commodities and nutrients in the
272 world⁵⁰. Taken as a whole, the expansion and site-specific tailoring of human-
273 augmented farming ecosystems has the potential to uplift the baseline of multiple
274 ecosystem services and provide fundamental measures to cope with growing food
275 demand and for proactive adaptation of various crop portfolio to climate change. It
276 may in the long run introduce a human-driven form of resilience in biosphere integrity
277 along with the expansion of essential human activities, by involving increasing
278 population as a positive driver of biodiversity in Anthropocene^{14, 30}.

279
280
281
282
283

284 **Box 1. Integrated model of physiological and ecological optima (IMPEO)³⁰.**
285 The physiological optimum is the basis of monoculture optimization in agronomy,
286 which is generally expressed as a unimodal distribution along the environmental
287 gradient (Fig 1 (a)). In actual ecological situations, however, isolated growth is not
288 fully attained and mixed communities are prevalent, which results in diverse shifting,
289 division, and modification of the growth curve leading to the emergence of ecological
290 niches (Fig 1 (b)). Random harvesting from various environments asymptotically
291 converges the mean productivity to a normal distribution under the mean
292 environmental conditions of the samples (Fig 1 (c)). According to the nature of
293 competition with other species, the plants can qualitatively be classified as those with
294 central or marginal competence (orange and blue distributions, respectively, in Fig 1).
295 Such differences generally produce competitive loss and symbiotic gain of
296 productivity, and both contribute to the total overyielding in mixed communities
297 (green distribution in Fig 1 (c)).
298 The contribution of symbiotic gain to the total overyielding in mixed polyculture
299 could become increasingly significant as the mean environment shifts from a
300 physiologically favorable condition (yellow background) to the marginal ranges
301 (orange background), and create new stretches of arable land in harsh conditions
302 where little monoculture growth can be expected (red background).
303 See the Supplementary Information and Figure 1 of the Extended Data for the
304 multi-dimensional version of IMPEO.
305
306

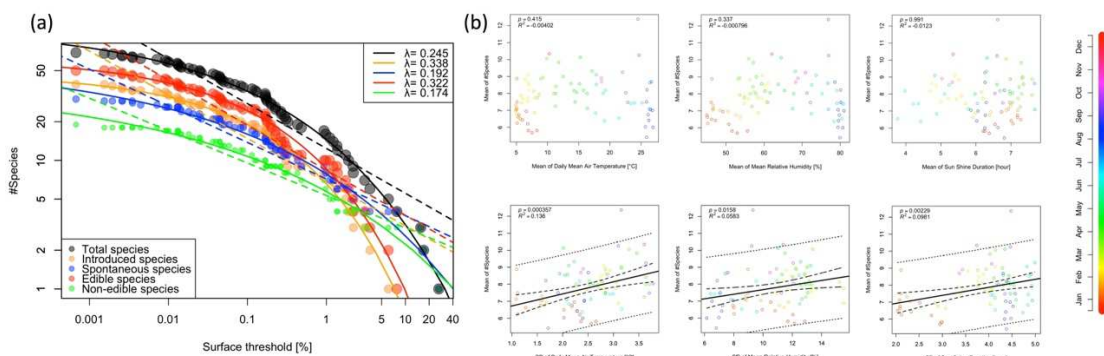


307
 308 **Fig 1. Relationship between physiological and ecological optima and the total**
 309 **effect of overyielding.** (a) y-axis: examples of physiologically optimum isolated
 310 growth rate versus x-axis: environmental parameters such as temperature,
 311 precipitation, sunlight, etc. (b) y-axis: primary productivity of various ecological
 312 niches in the same environment (x-axis) but mixed communities. (c) Top: random
 313 sampling from various niches in (a) (blue and orange dashed lines) and (b) (blue and
 314 orange solid lines) converges to normal distributions via the central limit theorem, their
 315 frequencies correspond to mean productivity measures such as harvest rate (y-axis)
 316 under averaged environmental conditions (x-axis). The overall productivity (green
 317 line) includes the productivities of plants of both growth-rate types. (c) Bottom:
 318 Effects of symbiotic gain (blue line and arrows) and competitive loss (orange line and
 319 arrows) of plants with marginal and central competence, respectively, measured as the
 320 land equivalent ratio (LER) on the scale of $LER' := \log(\log(LER) + 1)$. The main
 321 components of the total overyielding (green line) transit from centrally to marginally
 322 competent species as the environment shifts from the physiological optimum (yellow
 323 background) to marginal (orange background) and monoculture intolerant ranges (red
 324 background).
 325
 326



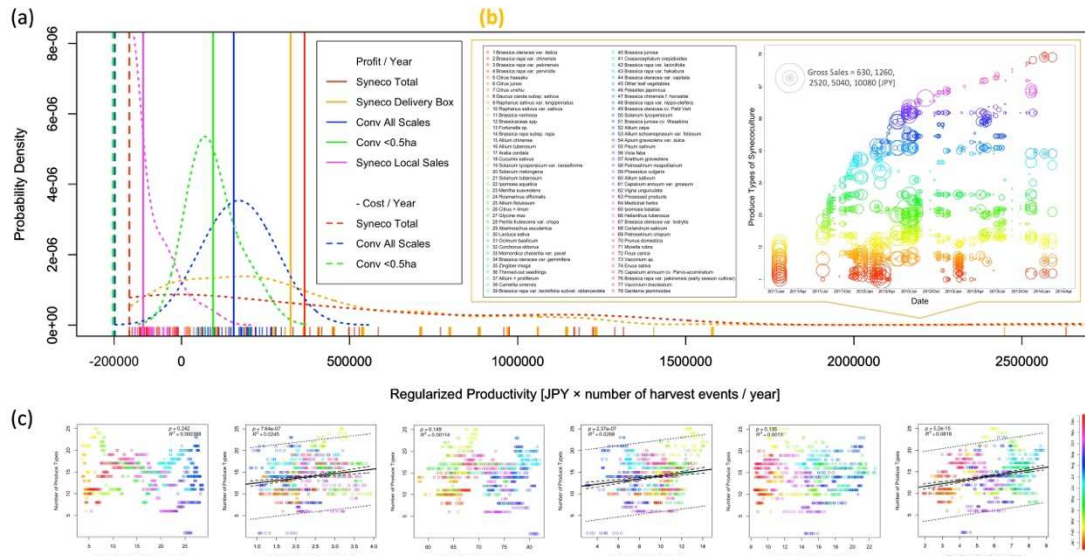
327
 328 **Fig 2. Studied synecoculture fields A (a1-a4), B (b1-b2), and C (c1-c5).** (a1-a4)
 329 Initial vegetation stages during the second year of crop species introduction from bare
 330 land in the temperate zone, in Oiso, Japan. After the construction of furrows in
 331 January, pictures show the transition of vegetation in (a1) early February, (a2) early
 332 May, (a3) late August, and (a4) late October. (b1) Pilot farm production experiment in
 333 the temperate zone, in Ise, Japan. Typical mixed polyculture state that augments
 334 diversity and productivity of vegetables in November is shown, with (b2) an example
 335 of the products packed in a delivery box. (c1-c5) Reversal of the regime shift in the
 336 semi-arid tropics, in Mahadaga, Burkina Faso. (c1) The control plot with no
 337 intervention remained bare for three years, while (c2) the introduction of 150 edible
 338 species established vigorous ecosystems including (c3) a strategic combination of
 339 crops with high density and vertical diversity. Partial regeneration of grass is observed
 340 in the background of (c1), which appears to be a positive effect from the neighboring
 341 synecoculture field (c2-c3). (c4) Little organic matter is visible in the image of the
 342 topsoil of the control plot, which is in contrast to (c5) showing the elaborated porous
 343 structure in the synecoculture plot.

344
 345

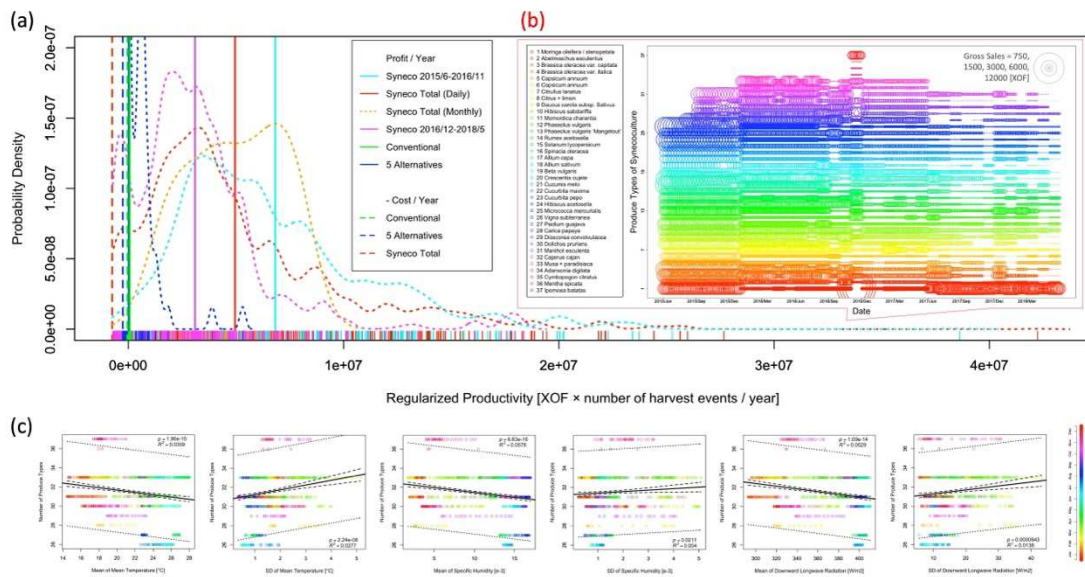


346
 347 **Fig 3. Spatial distribution and positive correlation with environmental variances**
 348 **in the initial stage of ecologically optimum crop growth in the temperate zone**
 349 **(field A).** The initial-stage experiment in Oiso, Japan (Fig 2 (a1-a4)) shows that (a) the
 350 estimated inverse cumulative distribution of the number of different plant species
 351 versus the percentage of the surface they occupy is closer to a power-law distribution
 352 that reflects symbiotic interactions $\lambda = 0$ than to an exponential distribution that
 353 merely reflects competition for resources $\lambda = 1$. (b) There exist positive correlations

354 between the mean number of observed species and the variance of meteorological
 355 parameters over the 30 days preceding the daily plot observation. There is no
 356 observable correlation with the means of the meteorological parameters. Mean plant
 357 species diversity versus mean and variance of three meteorological parameters are
 358 plotted with circles following the color gradient depicting the date. Black solid line:
 359 linear regression with less than 5% significance; dashed line: linear regression with
 360 95% confidence; dotted line: linear regression with prediction intervals.
 361
 362



363 **Fig 4. Productivity of synecoculture experiment in the temperate zone (field B).**
 364 The four- year production experiment in Ise, Japan shows (a) a power-law distribution
 365 of product sales with (b in the orange rectangle) asynchronous harvests of 78 kinds of
 366 crop. The x-axis of (a) represents sales of each product in synecoculture on 1,000 sq.m
 367 (regularized productivity is daily and species-wise productivity in terms of Japanese
 368 yen (JPY) multiplied by the number of harvest events per year for synecoculture or
 369 yearly reported profit for conventional methods), both with an offset of total costs in
 370 order to compare the yearly mean profits (vertical solid lines) and costs (vertical
 371 dashed lines) summed as positive and negative values, respectively (see Methods).
 372 The dotted lines on the y-axis represent the estimated probability distributions for
 373 each production category based on the data shown as the rug plots along the x-axis. In
 374 (b) left, the 78 academic names of total synecoculture products are shown as a list
 375 with a color gradient, and the associated numbers define the value of the y-axis in (b)
 376 right, in which the sales for each product according to date on the x-axis is represented
 377 as the diameter of the circle with the same color gradient as the list.
 378 The correlational analysis in (c) shows significant positive correlations between the
 379 number of produce types from synecoculture and meteorological variances for each
 380 30-day interval. There was no significant correlation with the mean of the
 381 meteorological parameters.
 382
 383 Harvested crop diversity versus mean or variance of three meteorological
 384 parameters is plotted as circles following the color gradient of the date. Black solid
 385 line: linear regression with less than 5% significance; dashed line: linear regression
 386 with 95% confidence; dotted line: linear regression with prediction intervals.



389
390 **Fig 5. Productivity of synecoculture experiment in the tropical semi-arid zone**
391 **(field C).** The three-year production experiment in Mahadaga, Burkina Faso shows a
392 power-law distribution of product sales with (b in the red rectangle) asynchronous
393 harvests of 37 kinds of crop. The x-axis of (a) represents sales of each product for
394 synecoculture and for five alternative farming methods that were simultaneously
395 tested on 500 sq.m (regularized productivity is daily and species-wise productivity in
396 terms of West African CFA franc (XOF) multiplied by the number of harvest events
397 per year for synecoculture and five alternative farming methods or yearly reported
398 profit for the conventional methods), both with an offset of total costs in order to
399 compare the yearly mean profits (vertical solid lines) and costs (vertical dashed lines)
400 summed as positive and negative values, respectively (see Methods). The dotted lines
401 represent the estimated probability distributions for each production category on the
402 y-axis based on the data shown by the rug plots along the x-axis. The total
403 productivity of synecoculture (red line and distribution) is shown on a monthly
404 aggregated scale (orange distribution) and in the two periods before (cyan line and
405 distribution) and after (magenta line and distribution) November 2016, which was the
406 turning point of market accessibility (see Methods). In (b) left, the 37 academic names
407 of total synecoculture products are shown as a list with a color gradient, and the
408 associated numbers define the value of the y-axis in (b) right, in which the sales of
409 each product according to date on the x-axis is represented as the diameter of the
410 circle with the same color gradient as the list.
411 The correlational analysis in (c) shows significant positive correlations between the
412 number of produce types from synecoculture and meteorological variances for each
413 14-day interval. There are also significant negative correlations with the means of the
414 meteorological parameters. Harvested crop diversity versus mean or variance of three
415 meteorological parameters is plotted as circles following the color gradient of the
416 year's date. Black solid line: linear regression with less than 5% significance; dashed
417 line: linear regression with 95% confidence; dotted line: linear regression with
418 prediction intervals.

419
420
421

Methods

422 Methods Summary

423 We developed a theory that connects the differing definitions of productivity of
424 monoculture-based optimization in agronomy and mixed community-based growth in
425 ecology, which defines the protocol of synecological farming (synecoculture) as an
426 extreme typology of plant food production based on self-organized ecological niches
427 of a highly diverse community of crops mixed with other spontaneous vegetation.
428 Out of 60+ implementations, three small-scale plots representative of the good
429 practice for smallholders were chosen in Japan and Burkina Faso, which were
430 prepared following the protocol of synecoculture, and maintained without the use of
431 tillage, fertilizers, or agrochemicals.

432 The species-wise surface was measured for a year in a harvest-free plot in
433 Japan (field A) and was analyzed whether the vegetation patch pattern followed a
434 power law that reflects symbiotic interaction between plants, or an exponential
435 distribution based merely on the competition for resources.

436 Additionally, two production farms in Japan (field B) and Burkina Faso (field
437 C) were chosen based on the completeness of three or more years of data on its
438 productivity and cost. A wide variety of species-wise product sales was recorded and
439 the statistical properties of the time series were analyzed in comparison with official
440 statistics on productivity and the cost of conventional market gardening and other
441 parallelly tested farming methods.

442 In all experiments, we compared the mean and variance parameters of
443 meteorological records of the finest satellite open data with the observed plant
444 diversity and analyzed statistical correlation that represented the biodiversity
445 response to a changing environment during the growth period.
446

447 Simulation of the integrated model of physiological and ecological optima 448 (IMPEO): Box 1 and Fig 1.

449 Based on ref. 29, we simulated a typical scenario of overyielding with a mixed
450 polyculture of two plant species. First, let us describe the unimodal distribution of
451 physiological growth of two species with the same physiological optimum range (Fig 1
452 (a)). We define this distribution as $U(Env; \nu_p)$ with an environmental parameter
453 Env and its physiologically optimum value ν_p giving the maximum growth rate. The
454 emerging ecological niches through interactions between the two species and the
455 environment have several typologies, such as shifting and division, and other
456 modifications of the growth curve, which are impossible to simulate precisely (Fig 1
457 (b)). Nevertheless, we will assume that there are qualitatively two different types of
458 niche differentiation dynamics: 1) One plant type shows the superiority in growth of
459 the physiological optimum to the other species (i.e., central competence expressed as
460 the orange distributions in Fig 1 (b)); 2) The other plant type shows superiority in
461 regard to growth in the marginal condition relative to the physiologically favorable
462 range (i.e., marginal competence expressed as the blue distributions in Fig 1 (b)).

463 Let us describe the diverse ecological niches as $GR_c = EN_c(Env; \nu_c, \sigma_c)$ for
464 centrally competent species and $GR_m = EN_m(Env; \nu_m, \sigma_m)$ for marginally

465 competent species under the following assumptions, $v_c = v_m = v_p$ and $\sigma_c < \sigma_m$,
466 where GR_c and GR_m stand for the growth rates, Env is an environmental
467 parameter, and v_c, v_m and σ_c, σ_m are the means and standard deviations of Env
468 for centrally and marginally competent species, respectively. For simplicity, we set
469 the same surface ratio between centrally and marginally competent species, but the
470 model is valid for any arbitrary ratio of mixed polyculture.

471 Random harvesting from all environments in those niches (i.e., random
472 sampling from the growth rate distributions GR_c and GR_m) results in a normal
473 distribution of mean productivity through the central limit theorem, such that
474 $HR_c \sim N(E[Env]; v_c, \sigma_c)$ and $HR_m \sim N(E[Env]; v_m, \sigma_m)$, where $N(\cdot; v, \sigma)$ is a
475 normal distribution with mean v and standard deviation σ , HR_c and HR_m
476 respectively represent the harvest rate of centrally and marginally competent species
477 of the mean environmental parameter $E[Env]$ over the sampling. We can also obtain
478 the mean monoculture productivity $U' \sim N(E[Env]; v_p, \sigma_p)$ by using the same
479 sampling method, which results in $\sigma_c < \sigma_p < \sigma_m$. In Fig 1 (c) top, HR_c is depicted
480 as an orange line, HR_m as a blue line, and $HR_c + HR_m$ as a green line. The
481 parameters $\sigma_p = 20$, $\sigma_c = 19.7$, and $\sigma_m = 40$ were typical values chosen to
482 illustrate the effects of competitive loss (orange arrows) and symbiotic gain (blue
483 arrows). In Fig 1 (c) bottom, the land equivalent ratio (LER)⁵¹ is the value calculated
484 between the mean monoculture productivity U' and its polyculture counterparts
485 HR_c and HR_m , as $LER = \frac{HR_c + HR_m}{U'}$ (green line), and its species-wise components
486 $\frac{HR_c}{U'}$ (orange line) and $\frac{HR_m}{U'}$ (blue line). These LER components are depicted on a
487 scale of $LER' := \log(\log(LER) + 1)$, where the straight dotted black line is the
488 separatrix $LER' = 0$ between symbiotic gain (upper part, $LER' > 0$) and
489 competitive loss (lower part, $LER' < 0$).

490
491

492 **Implementation of synecological farming (synecoculture) in Oiso and Ise, Japan** 493 **and Mahadaga, Burkina Faso (Fig 2).**

494 Among more than 60 social implementation sites supported by scientific research of
495 Sony CSL and UniTwin UNESCO CS-DC program during 2010-2023 (more than 50
496 in the Sahel⁴⁴ and 10 in Japan³⁴), we screened three representative cases that satisfied
497 the following conditions:

- 498 1) One experimental field of the initial succession stage in Japan with a
499 surface cover record of each vegetation without harvest (Field A)
- 500 2) One production site in Japan, which had sufficient diversity of crops and
501 market access, and complete sales and cost records for three or more years
502 (Field B)
- 503 3) One production site in the Sahel, which had sufficient diversity of crops
504 and market access, and complete sales and cost records for three or more
505 years (Field C)

506

507 These three sites established the highly biodiverse ecosystems following the
508 protocol of synecoculture farming method, started from bare ground^{24,52,53}:

- 509 • Field A: From January 2010 to December 2011, randomly mixed

- 510 communities of 52 edible plant species and other naturally occurring species
511 on 420 sq.m without harvesting or watering and little weed maintenance in
512 Oiso, Japan (GPS coordinates in decimal degrees: 35.31675, 139.32515).
- 513 • Field B: From April 2008, a preliminary observation of ecological niches of
514 various plant species; from June 2010 to May 2014, a strategically mixed
515 association of 133 edible plant species and other naturally occurring species
516 on a commercial farm of 1,000 sq.m with harvesting and occasional watering
517 and weed maintenance in Ise, Japan (GPS coordinates in decimal degrees:
518 34.53022, 136.6873).
 - 519 • Field C: After the introduction of seeds and seedlings on March 2015, from
520 June 2015 to May 2018, a strategically mixed association of 150 edible plant
521 species on a commercial farm of 500 sq.m with harvesting, watering, and a
522 small amount of weed maintenance in Mahadaga, Tapoa province, Burkina
523 Faso (GPS coordinates in decimal degrees: 11.72328, 1.76136).

524 For all implementations, only seeds and seedlings and necessary water as specified
525 were introduced in the fields. No synthetic and organic fertilizers, no agrochemicals
526 or other phytosanitary products, no ground cover materials, and no other amendments
527 were used. No agricultural machinery was used, except for a small handy mower in
528 the field B. No external financial support was given to the commercial synecoculture
529 farms (field B and C).

530
531

532 **Surface distribution analysis and correlation analysis between species diversity** 533 **and meteorological parameters at the synecoculture field A (Fig 3).**

534 The covering surface of each plant species at low ground level in field A was
535 measured with 2-step visual analog scale method (an extension of the traditional
536 Brown-Blanquet method into percentile resolution to assess the field vegetation
537 cover)³³ on 80 sections measuring 2 sq.m each, 22 times at an interval of 1 week to
538 1.5 months (about once every 2.3 weeks on average) at a frequency depending on
539 the degree of growth during January – December 2011 [Supplementary Data 1]. The
540 observed plant species were categorized into 1) introduced crop species and 2)
541 naturally occurring spontaneous species, which were also parallelly labeled as 3)
542 edible species that were utilized and 4) non-edible species that were not yet utilized
543 as synecoculture products.

544 In Fig 3 (a), the inverse cumulative distribution of the number of different
545 species is plotted with respect to the minimum threshold of yearly averaged covering
546 surface ratio. Theoretical models show that the size distribution of self-organized
547 vegetation surface tends to an exponential distribution that reflects competition
548 between plants for resources, but that it tends to a power-law distribution when there
549 is locally symbiotic relationship^{28,29}. This assumption applies to the analysis of both
550 the inverse-cumulative and non-cumulative distributions, since power-law and
551 exponential functions are conserved under the transformation from a probability
552 density to its cumulative distribution. The experiment in the field A focused on
553 measuring the relative degree of contribution between local symbiotic interactions
554 and resource competition at the inter-species level (i.e., symbiotic gain and
555 competitive loss in IMPEO) through an analysis of the species-wise averaged surface
556 distribution. We devised an integrative model to evaluate the goodness of fit between

557 the power-law and exponential distributions:

558
$$\log Y = A \cdot \text{BoxCox}(X, \lambda) + B$$

559 where $\text{BoxCox}(X, \lambda) = \begin{cases} \frac{X^\lambda - 1}{\lambda} & (1 \geq \lambda > 0) \\ \log X & (\lambda = 0) \end{cases}$ is the Box-Cox transformation with a

560 continuous parameter $1 \geq \lambda \geq 0$, which converges to an exponential distribution
561 $\log Y = A \cdot X - A + B$ in the $\lambda = 1$ case and a power-law distribution $\log Y = A \cdot$
562 $\log X + B$ in the $\lambda = 0$ case. The fitting was performed using the `bcPower()` and
563 `nls()` functions in R⁵⁴.

564 In Fig 3 (b), mean species diversity in daily observed sections versus the mean
565 and standard deviation of major meteorological parameters during the past 30 days
566 from the observation (substantial growth period of the crops in the field) are plotted.
567 Complete plots are shown in Figure 2 of the Extended Data. Eight parameters
568 representing major environmental factors for plant growth (temperature, humidity, and
569 sunlight) in an area measured at a daily 1-km grid resolution from December 2010 to
570 December 2011 were obtained from the Agro-Meteorological Grid Square Data
571 System, NARO (<https://amu.rd.naro.go.jp/>)⁵⁵: daily mean air temperature, daily
572 maximum air temperature, daily minimum air temperature, daily precipitation
573 (reanalysis), mean relative humidity, global solar radiation, downward long-wave
574 radiation, and sunshine duration. The correlation analysis was performed using the
575 `lm()` function in R⁵⁴.

576
577

578 **Productivity analysis and correlation analysis of species diversity and** 579 **meteorological parameters of synecoculture field B (Fig 4).**

580 78 kinds of vegetable and fruit products were harvested from field B and sold as
581 delivery boxes from January 2011 to February 2014 at a price rate of 315 JPY per 100
582 g, which is approximately equivalent to the rate for certified organic products (about
583 1.5 times higher than the price of conventional farm products) in the same region
584 [Supplementary Data 2]. From June 2010 to May 2014, other edible plant products,
585 seeds and seedlings were also occasionally harvested and sold on-site, including as
586 ingredients for a local restaurant; the data are summarized for each month
587 [Supplementary Data 3]. The principal cost was comparable to that of the conventional
588 methods and comprised the cost of seeds and seedlings [Supplementary Data 4].

589 Yearly average data of productivity (gross sales in JPY) and material costs
590 (seeds and seedlings, fertilizers and other amendments, materials such as plastic
591 mulch, and machinery such as a tractor) of open-field conventional market gardening
592 during 2010-2014 were obtained from the online database provided by the Ministry of
593 Agriculture, Forestry and Fisheries in Japan⁵⁶. These datasets were converted into
594 amounts per 1,000 sq.m. The probability density functions shown in Fig 4 (a) were
595 numerically estimated using the `density()` function in R⁵⁴.

596 To compare the yearly summed productivity of the conventional methods and
597 with the daily recorded productivity of synecoculture, the scale of the x-axis of Fig 4
598 (a) is each unit sale multiplied by the number of harvest events per year. The
599 conventional data consists of the yearly mean gross sales $X_c = \sum_{i=1}^n c_i$ that comprise
600 those of n harvest events $\{c_i\}$, which are not explicitly shown in the dataset. n is
601 usually small (a few times per year for each crop), and $\{c_i\}$ follows a normal

602 distribution because it is based on a large sum of simultaneous harvests of monoculture
603 crops; therefore, X_c is a good representative value of $\{c_i\}$. One can compare X_c
604 with the yearly summed gross sales of synecoculture $X_s = \sum_{i=1}^m s_i$ based on the
605 record of m harvest events $\{s_i\}$ in daily and species-wise resolution, which is shown
606 as vertical solid lines and rug plots in Fig 4 (a). In synecoculture, m is large (yearly
607 average, $m = 285$ for the field B and $m = 3619$ for the field C), and $\{s_i\}$ follow a
608 power-law distribution (also plotted in Figure 5 of the Extended Data). Therefore, $\{s_i\}$
609 contains a large deviation from X_s . In order to plot $\{s_i\}$ on a compatible scale with
610 X_c and X_s , we need to define the regularized productivity $r_i = m \cdot s_i$ (daily and
611 species-wise productivity s_i multiplied by the number of harvest events m on a
612 yearly scale), because in that way the mean value of $\{r_i\}$ coincides with X_s , i.e.,
613 $X_s = \sum_{i=1}^m s_i = \sum_{i=1}^m m \cdot s_i / m = \frac{1}{m} \sum_{i=1}^m r_i$, regardless of the frequency of harvest
614 events. The same scale applies to the yearly costs that are expressed as a negative
615 offset to gross sales, which is depicted with the vertical dashed lines in Fig 4 (a).

616 The correlation between the number of produce types (product diversity
617 measured by the number of different species) sold as delivery box and the mean and
618 standard deviation of eight major meteorological parameters⁵⁵ (same as in the field A
619 experiment) for each 30-day interval was analyzed. Typical results are shown in Fig 4
620 (c); complete plots are shown in Figure 3 of the Extended Data.

621
622

623 **Productivity analysis and correlation analysis between species diversity and** 624 **meteorological parameters of synecoculture field C (Fig 5).**

625 Products from 37 plant species in field C were harvested and sold at a local market
626 from June 2015 to May 2018^{53,57,58}. The price rate was set to those of organic products
627 (about two times higher than conventional products) from June 2015 to May 2017,
628 and to the prices of conventional products from June 2017 to May 2018, because of
629 deterioration of local security situation and consequent loss of customers.

630 Five alternative methods that aim for sustainable farming were also tested
631 alongside the synecoculture production during the same period, namely 1: a system of
632 rice intensification and trees, 2: conservation agriculture, 3: permaculture, 4: bio-
633 intensive market gardening, and 5: traditional market gardening. We obtained the
634 gross sales of synecoculture sales at a daily resolution [Supplementary Data 5] and
635 those of the five alternative methods in terms of the monthly aggregated sum
636 [Supplementary Data 6], together with the monthly installation, materials and working
637 costs [Supplementary Data 7].

638 Conventional market gardening data based on the estimation of ten crops in
639 Burkina Faso was obtained from a Food and Agriculture Organization of the United
640 Nations (FAO) document⁵⁹ on standards of gross sales and costs, which included only
641 installation and water costs and excluded other operation costs such as seeds and
642 seedlings, fertilizer and phytosanitary products, and materials and working costs.

643 Datasets of gross sales and costs of the five alternative and conventional
644 methods were converted into amounts per 500 sq.m. The probability density
645 functions in Fig 5 (a) were numerically estimated using the density() function in R⁵⁴.
646 The x-axis in Fig 5 (a) conforms to that of Fig 4 (a).

647 In regard to Fig 5 (c), satellite meteorological data corresponding to the field C

648 at a daily 19.2-km grid resolution was obtained from (<http://clim->
649 [engine.appspot.com/](http://clim-engine.appspot.com/))⁶⁰. From which, 19 major parameters related to plant growth
650 were taken from the Climate Forecast System (CFS) Reanalysis dataset of the
651 National Centers for Environmental Prediction (NCEP): maximum temperature, mean
652 temperature, minimum temperature, potential evaporation, precipitation, specific
653 humidity, maximum specific humidity, minimum specific humidity, 5-cm soil
654 moisture, 25-cm soil moisture, 70-cm soil moisture, 150-cm soil moisture, net
655 radiation, downward shortwave radiation, upward shortwave radiation, downward
656 longwave radiation, upward longwave radiation, latent heat flux, and sensible heat
657 flux.

658 The correlation between the number of produce types (product diversity
659 measured by the number of different species) and the means and standard deviations of
660 the meteorological parameters for each 14-day interval (a substantial period of growth
661 of crops in the field) were analyzed. Typical results are illustrated in Fig 5 (c); the
662 complete plots are shown in Figure 4 of the Extended Data.

663
664

665 **Estimation of harvest biomass from product sales**

666 Although the land equivalent ratio (LER)⁵¹ is used to evaluate polyculture
667 productivity, it is not suitable for evaluating highly diverse mixed polycultures for two
668 reasons:

- 669 1. For any probability distribution with the mean ν and standard deviation σ ,
670 the effect of fluctuations expressed as a ratio $\frac{\nu \pm \sigma}{\nu \pm \sigma}$ is not symmetric with
671 respect to the standard ratio $\frac{\nu \pm 0}{\nu \pm 0} = 1$, which results in the LER having a
672 positive bias; e.g., $\left(\frac{\nu + \sigma}{\nu + \sigma} + \frac{\nu - \sigma}{\nu + \sigma} + \frac{\nu + \sigma}{\nu - \sigma} + \frac{\nu - \sigma}{\nu - \sigma}\right) / 4 = \nu^2 / (\nu^2 - \sigma^2) > 1$.
673 Therefore, even if the monoculture and polyculture productivities are equal,
674 the effect of fluctuation in LER gives a positive bias to polyculture.
- 675 2. Actual monoculture productivity data is a weighted sum of many monoculture
676 crops^{56,59}, which is equivalent to a polyculture based on a mosaic of different
677 monoculture surfaces. Therefore, the proportion of each crop surface within a
678 given social-ecological context affects the overall productivity, which is not
679 considered to be a realistic constraint in LER.

680 To overcome this pitfall, we defined the relative biomass ratio (BR) that
681 represents the community-based land equivalent ratio as follows:

$$682 \quad BR := \frac{\sum_{i=1}^k X_i}{\sum_{j=1}^l Y_j}$$

683 Where X_i is the mixed polyculture yield ($k > 1$ crops are mixed together on the
684 same surface) of the i th crop, and Y_j is the mosaic polyculture yield (a
685 combination of separate monocultures with $l > 1$ different crops on the same
686 surface area) of the j th crop. Note that BR coincides with $LER := \sum_{i=1}^k \frac{X_i}{U'}$ in
687 the IMPEO of one or more crops with the same physiological growth curve U' .

688 In the case that k crops for P_i are included in the l crops of Q_j , which
689 is the case for field B, it is possible to calculate the BR of the mixed polyculture
690 products using the sales data weighted with the per-price weight of each crop:

691
$$BR := \frac{\sum_{i=1}^k P_i \cdot V_i}{\sum_{j=1}^l Q_j \cdot W_j}$$

692 Where P_i and Q_j are the productivity measured by the sale price, V_i and W_j
 693 are product biomass per unit price for each crop ($X_i = P_i \cdot V_i$ and $Y_j = Q_j \cdot W_j$).
 694 In this study, the price rate R of Synecoculture products are set as $R := \frac{W_i}{V_i} \cong 1.5$
 695 in field B. For field C, $R \cong 2.0$ and $R \cong 1.0$ for the first two years and the third
 696 year, respectively.

697 In sufficiently diverse sets of crops, the average product biomass per
 698 price defined as $V := \frac{\sum_{i=1}^k P_i \cdot V_i}{\sum_{i=1}^k P_i}$ and $W := \frac{\sum_{j=1}^l Q_j \cdot W_j}{\sum_{j=1}^l Q_j}$ converge to finite values, and
 699 their ratio converges to R , such that $\frac{W}{V} \approx R$. Using these relationships, the
 700 estimation of BR is obtained as follows:

701
$$BR \approx \frac{V \cdot \sum_{i=1}^k P_i}{W \cdot \sum_{j=1}^l Q_j} = \frac{\sum_{i=1}^k P_i / R}{\sum_{j=1}^l Q_j}$$

702 If k crops for P_i are not totally included in the l crops of Q_j , which is the
 703 case of field C, we considered the possible variable range of conventional productivity
 704 based on the median and 25th and 75th percentiles of productivity in l crops (see also
 705 Figure 6 (b2) of the Extended Data).

706 This estimated biomass does not include the biomass of the established
 707 ecosystem permanently present in the synecoculture field, such as trees and seedlings,
 708 naturally occurring non-edible plants, fallen leaves, stems after harvest, and highly
 709 developed root systems that are sources of soil organic matter.

710
 711

712 **Power-law fitting of surface distribution and harvest sales in Figure 5 of the**
 713 **Extended Data.**

714 The probability density (y-axis) of the following variables (x-axis) was estimated
 715 using the density() function in R and linearly fitted with a Pareto distribution $Y =$
 716 $\frac{ab^a}{x^{a+1}}$ on a double-logarithmic scale by using the lm() function in R⁵⁴.

717

718 Field A: Species-wise surface percentage data for 80 2-sq.m sections in the Oiso farm
 719 [Supplementary Data 1]. Surface data above 5% and the estimated probability density
 720 were used for the fitting.

721 Field B: Crop-wise daily sales data of the delivery box from the Ise farm
 722 [Supplementary Data 2]. Sales data above 1,000 JPY and the estimated probability
 723 density above 1.0e-7 were used for the fitting.

724 Field C: Crop-wise daily sales data of the Mahadaga farm [Supplementary Data 5].
 725 Sales data above 1,000 XOF and the estimated probability density above 1.0e-7 were
 726 used for the fitting.

727

728

729

730 **References**

731

- 732 1. Barnosky, A. D. et al. Approaching a state shift in Earth's biosphere. *Nature* **486**,
733 52-58 (2012).
- 734 2. Ripple, W. J. et al. World Scientists' Warning to Humanity: A Second Notice.
735 *BioScience* **67**, 1026–1028 (2017).
- 736 3. Díaz, S. et al. Pervasive human-driven decline of life on Earth points to the need
737 for transformative change. *Science* **366**, eaax3100 (2019).
- 738 4. Intergovernmental Science-Policy Platform on Biodiversity and Ecosystem
739 Services (IPBES). *Global assessment report on biodiversity and ecosystem services*
740 *of the Intergovernmental Science-Policy Platform on Biodiversity and Ecosystem*
741 *Services*. IPBES secretariat, Bonn, Germany (2019).
- 742 5. McDowell, N. G. et al. Pervasive shifts in forest dynamics in a changing world.
743 *Science* **368**, eaaz9463 (2020).
- 744 6. Ceballos, G., Ehrlich, P. R. & Raven, P. H. Vertebrates on the brink as
745 indicators of biological annihilation and the sixth mass extinction. *Proc.*
746 *Natl. Acad. Sci. USA* **117**, 13596-13602 (2020).
- 747 7. Sánchez-Bayo, F. & Wyckhuys, K. A. G. Worldwide decline of the
748 entomofauna: A review of its drivers. *Biol. Conserv.* **232**, 8-27 (2019).
- 749 8. Diaz, R. J. & Rosenberg R. Spreading dead zones and consequences
750 for marine ecosystems. *Science* **321**, 926-929 (2008).
- 751 9. Smith, P. et al. in *Climate Change 2014: Mitigation of Climate Change.*
752 *Contribution of Working Group III to the Fifth Assessment Report of the*
753 *Intergovernmental Panel on Climate Change* (eds Edenhofer, O. et al.) 2014:
754 *Agriculture, Forestry and Other Land Use (AFOLU)*. (Cambridge University Press,
755 2014).
- 756 10. Steffen, W. et al. Planetary boundaries: Guiding human development on a
757 changing planet. *Science* **347**, 1259855 (2015).
- 758 11. The Intergovernmental Panel on Climate Change (IPCC). *Global Warming of*
759 *1.5°C*. *Global Warming of 1.5°C. An IPCC Special Report on the impacts of global*
760 *warming of 1.5°C above pre-industrial levels and related global greenhouse gas*
761 *emission pathways, in the context of strengthening the global response to the*
762 *threat of climate change, sustainable development, and efforts to eradicate*
763 *poverty*. Masson-Delmotte, V. et al. (eds.) (2018).
- 764 12. Daszak, P., et al. *Workshop Report on Biodiversity and Pandemics of the*
765 *Intergovernmental Platform on Biodiversity and Ecosystem Services*. IPBES
766 secretariat, Bonn, Germany (2020).
- 767 13. Costanza, R. et al. Twenty years of ecosystem services: How far have we come
768 and how far do we still need to go? *Ecosyst. Serv.* **28**, 1-16 (2017).
- 769 14. Funabashi, M. Human augmentation of ecosystems: objectives for food
770 production and science by 2045. *NPJ Sci. Food* 2018, 2: 16 (2018).
- 771 15. Erb, K. -H. et al. Exploring the biophysical option space for feeding the world
772 without deforestation. *Nat. Commun.* **7**, 11382 (2016).
- 773 16. Bastin, J. -F. et al. The global tree restoration potential. *Science* **365**, 76-79 (2019).
- 774 17. Sattari, S. Z., Bouwman, A. F., Rodríguez, R. M., Beusen, A. H. W. & van
775 Ittersum, M. K. Negative global phosphorus budgets challenge sustainable
776 intensification of grasslands. *Nat. Commun.* **7**, 10696 (2016).
- 777 18. Machmuller, M. B. et al. Emerging land use practices rapidly increase soil organic
778 matter.
779 *Nat. Commun.* **6**, 6995 (2015).

- 780 19. Veldman, J. W. et al. Comment on “The global tree restoration potential”.
781 *Science* **366**, eaay7976 (2019).
- 782 20. Lesiv, M. et al. Estimating the global distribution of field size using
783 crowdsourcing. *Glob. Chang. Biol.* **25**, 174-186 (2019).
- 784 21. Ending hunger: science must stop neglecting smallholder farmers. *Nature* **586**,
785 336 (2020).
- 786 22. Altieri, M. A. Agroecology: the science of natural resource management for poor
787 farmers in marginal environments. *Agr. Ecosyst. Environ.* **93**, 1-24 (2002).
- 788 23. Tokoro, M. Open Systems Science: A Challenge to Open Systems Problems.
789 in *First Complex Systems Digital Campus World E-Conference 2015*
790 (Bourguine, P., Collet, P. & Parrend, P. eds.) pp. 213–221 (Springer
791 International Publishing, Switzerland, 2017).
- 792 24. Funabashi, M. et al. Foundation of CS-DC e-laboratory: Open Systems
793 Exploration for Ecosystems Leveraging. in *First Complex Systems Digital*
794 *Campus World E-Conference 2015* (Bourguine, P., Collet, P. & Parrend, P.
795 eds.) pp. 351-374 (Springer International Publishing, Switzerland, 2017).
- 796 25. Schork, N. J. Personalized medicine: Time for one-person trials. *Nature* **520**,
797 609-611 (2015).
- 798 26. Planetary Health Alliance <https://www.planetaryhealthalliance.org/>
- 799 27. Tilman, D. Diversity and productivity in a long-term grassland experiment.
800 *Science* **294**, 843-845 (2001).
- 801 28. Scanlon, T. M., Caylor, K. K., Levin, S. A. & Rodriguez-Iturbe, I. Positive
802 feedbacks promote power-law clustering of Kalahari vegetation. *Nature*
803 **449**, 209-212 (2007).
- 804 29. Kéfi, S. et al. Spatial vegetation patterns and imminent desertification in
805 Mediterranean arid ecosystems. *Nature* **449**, 213-217 (2007).
- 806 30. Funabashi, M. Synecological farming: Theoretical foundation on biodiversity
807 responses of plant communities. *Plant Biotechnol.* **32**, 1–22 (2016).
- 808 31. Funabashi, M. Augmentation of plant genetic diversity in Synecoculture:
809 theory and practice in temperate and tropical zones. in *Genetic Diversity in*
810 *Horticultural Plants* (Nandwani, D. eds.) pp.3-46 (Springer International
811 Publishing, Switzerland, 2019).
- 812 32. Smith, J., Yeluripati, J., Smith, P. & Nayak, D. R. Potential yield challenges to
813 scale-up of zero budget natural farming. *Nat. Sustain.* **3**, 247-252 (2020).
- 814 33. Lange, M. et al. Plant diversity increases soil microbial activity and soil carbon
815 storage.
816 *Nat. Commun.* **6**, 6707 (2015).
- 817 34. Funabashi, M. Synecological farming for mainstreaming biodiversity in
818 smallholding farms and foods: implication for agriculture in India. *Indian J.*
819 *Plant Genet. Resour.* **30**, 99–114 (2017).
- 820 35. Kéfi, S. et al. Early Warning Signals of Ecological Transitions: Methods
821 for Spatial Patterns. *PLoS One* **9**, e92097 (2014).
- 822 36. IIED & UNEP-WCMC. *Mainstreaming biodiversity and development:*
823 *guidance from African experience 2012-17*. IIED, London. (2017).
- 824 37. Rippke, U. et al. Timescales of transformational climate change adaptation
825 in sub-Saharan African agriculture. *Nat. Clim. Chang.* **6**, 605-609 (2016).
- 826 38. Pecl, G. T. et al. Biodiversity redistribution under climate change: Impacts on
827 ecosystems and human well-being. *Science* **355**, eaai9214 (2017).

- 828 39. Springmann, M. et al. Options for keeping the food system within environmental
829 limits. *Nature* **562**, 519-525 (2018).
- 830 40. Berdugo, M., Kéfi, S., Soliveres, S. & Maestre, F. T. Plant spatial patterns
831 identify alternative ecosystem multifunctionality states in global drylands.
832 *Nat. Ecol. Evol.* **1**, 0003 (2017).
- 833 41. The Great Green Wall <https://www.greatgreenwall.org/>
- 834 42. Tilman, D. et al. Future threats to biodiversity and pathways to their prevention.
835 *Nature* **546**, 73-81 (2017).
- 836 43. de Bruyn, J. et al. Food composition tables in resource-poor settings: exploring
837 current limitations and opportunities, with a focus on animal-source foods in sub-
838 Saharan Africa. *Br. J. Nutr.* **116**, 1709-1719 (2016).
- 839 44. Tchilalo, P., Tindano, A., & Funabashi, M. (eds) *Actes du 6e Forum Africain sur la*
840 *Synécoculture / Proceedings of the 6th African Forum on Synecoculture (French-*
841 *English Version)*. Research and Education material of UniTwin UNESCO
842 Complex Systems Digital Campus, e-laboratory: Human Augmentation of
843 Ecosystems, No. 2 (2022)
- 844 45. Alexandratos, N. & Bruinsma, J. *World agriculture towards 2030/2050: the 2012*
845 *revision. ESA Working paper No. 12-03*. Rome, FAO. (2012).
- 846 46. Stephenson, P. J. et al. Unblocking the flow of biodiversity data for decision-
847 making in Africa. *Biol. Conserv.* **213**, 335-340 (2017).
- 848 47. Frelat, R. et al. Drivers of household food availability in sub-Saharan Africa
849 based on big data from small farms. *Proc. Natl. Acad. Sci. USA* **113**, 458-463
850 (2015).
- 851 48. Jaenicke, H., Ganry, J., Hoeschle-Zeledon, I. & Kahane, R. (eds.) *International*
852 *symposium on underutilized plants for food security, nutrition, income and*
853 *sustainable development*. Arusha, Tanzania. ISBN 978-90-66057-01-2 (2009)
- 854 49. Lowder, S. K., Scoet, J. & Raney, T. The number, size, and distribution
855 of farms, smallholder farms, and family farms worldwide. *World Dev.*
856 **87**, 16-29 (2016).
- 857 50. Herrero, M. et al. Farming and the geography of nutrient production for human
858 use: a transdisciplinary analysis. *Lancet Planet. Health* **1**, e33-e42 (2017).
- 859 51. Mead, R. & Willey, R. W. The concept of a 'land equivalent ratio' and
860 advantages in yields from intercropping. *Exp. Agric.* **16**, 217-228 (1980).
- 861 52. Funabashi, M. (editor) *Synecoculture Manual 2016 Version (English Version)*
862 Research and Education material of UniTwin UNESCO Complex Systems
863 Digital Campus, e- laboratory: Open Systems Exploration for Ecosystems
864 Leveraging, No.2. (2016).
- 865 53. Tindano, A. & Funabashi, M. (eds) *Proceedings of the 1st African Forum on*
866 *Synecoculture (English Version)*. Research and Education material of UniTwin
867 UNESCO Complex Systems Digital Campus, e-laboratory: Open Systems
868 Exploration for Ecosystems Leveraging, No.5. (2017).
- 869 54. R version 3.6.0 <https://www.r-project.org/>
- 870 55. Ohno, H., Sasaki, K., Ohara, G. & Nakazono, K. Development of grid square
871 air temperature and precipitation data compiled from observed, forecasted, and
872 climatic normal data. *Climate in Biosphere*, **16**, 71-79 (in Japanese with
873 English title) (2016).
- 874 56. MAFF e-stat <http://www.e-stat.go.jp/SG1/estat/List.do?lid=000001089733>
875 Ministry of Agriculture, Forestry and Fisheries of Japan

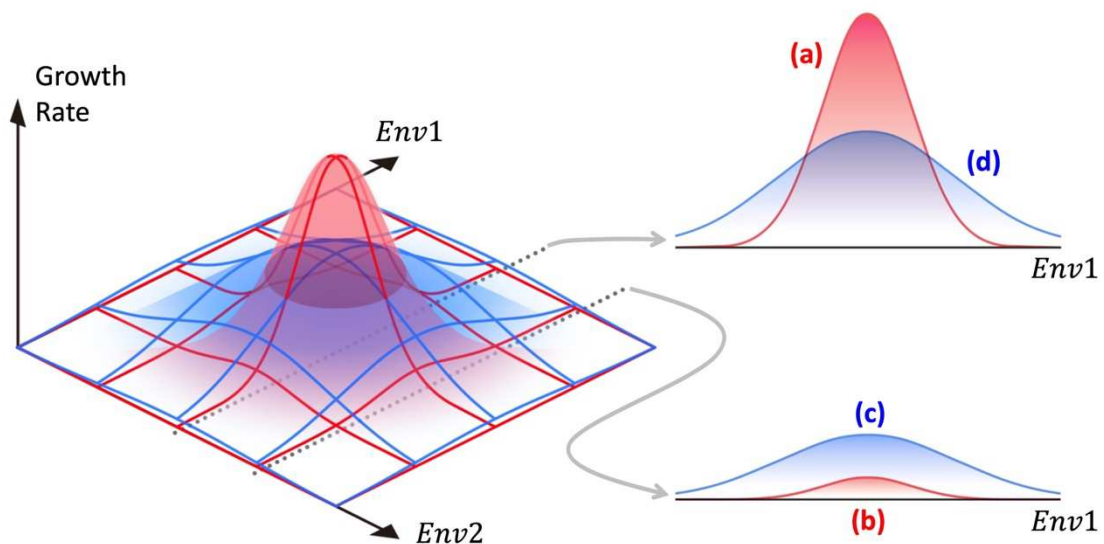
- 876 57. Tindano, A. & Funabashi, M. (eds) *Proceedings of the 2nd African Forum on*
877 *Synecoculture (English Version)*. Research and Education material of UniTwin
878 UNESCO Complex Systems Digital Campus, e-laboratory: Open Systems
879 Exploration for Ecosystems Leveraging, No.7. (2018).
- 880 58. Tindano, A. & Funabashi, M. (eds) *Proceedings of the 3rd African Forum on*
881 *Synecoculture (English Version)*. Research and Education material of UniTwin
882 UNESCO Complex Systems Digital Campus, e-laboratory: Open Systems
883 Exploration for Ecosystems Leveraging, No. 10. (2018).
- 884 59. FAO EASYPol. Analyse de la filière maraichage au Burkina Faso.
885 Ressources complémentaires, Module EASYPol 107
886 http://www.fao.org/docs/up/easypol/887/analyse-filiere-maraichage_107fr.pdf
887 (2017)
- 888 60. Huntington, J. L. et al. Climate Engine: cloud computing and visualization of
889 climate and remote sensing data for advanced natural resource monitoring and
890 process understanding. *Bull. Amer. Meteor. Soc.* **98**, 2397–2410 (2017).
891
- 892 [Supplementary Data 1] Supplementary Data 1: Surface data of field A experiment.
893 Will obtain doi after review
- 894 [Supplementary Data 2] Supplementary Data 2: Daily sales data of delivery box from
895 the field B. Will obtain doi after review
- 896 [Supplementary Data 3] Supplementary Data 3: Monthly on-farm sales data from the
897 field B. Will obtain doi after review
- 898 [Supplementary Data 4] Supplementary Data 4: Monthly cost data from the field B.
899 Will obtain doi after review
- 900 [Supplementary Data 5] Supplementary Data 5: Daily sales data of
901 Synecoculture from the field C. Will obtain doi after review
- 902 [Supplementary Data 6] Supplementary Data 6: Monthly sales data of five alternative
903 methods from the field C. Will obtain doi after review
- 904 [Supplementary Data 7] Supplementary Data 7: Monthly cost data from the field C.
905 Will obtain doi after review

Supplementary Information & Figures and Tables of the Extended Data

Multi-dimensional IMPEO

The environmental parameter in Fig. 1 is generally multi-dimensional. In such cases, the IMPEO is expressed with multi-dimensional normal distributions. Figure 1 of the Extended Data shows a typical representation of IMPEO with two-dimensional environmental parameters. Mean environmental parameters *Env1* and *Env2* that define the physiological optimum generally represent macroscopic culture conditions such as air temperature, precipitation, and solar radiation, but they can also be influenced by ecosystem dynamics and produce a variety of changes in microclimate such as soil temperature augmented by microbiological activities, soil moisture that depends on soil porosity, and actual luminosity on the leaf surface shaded by other plants.

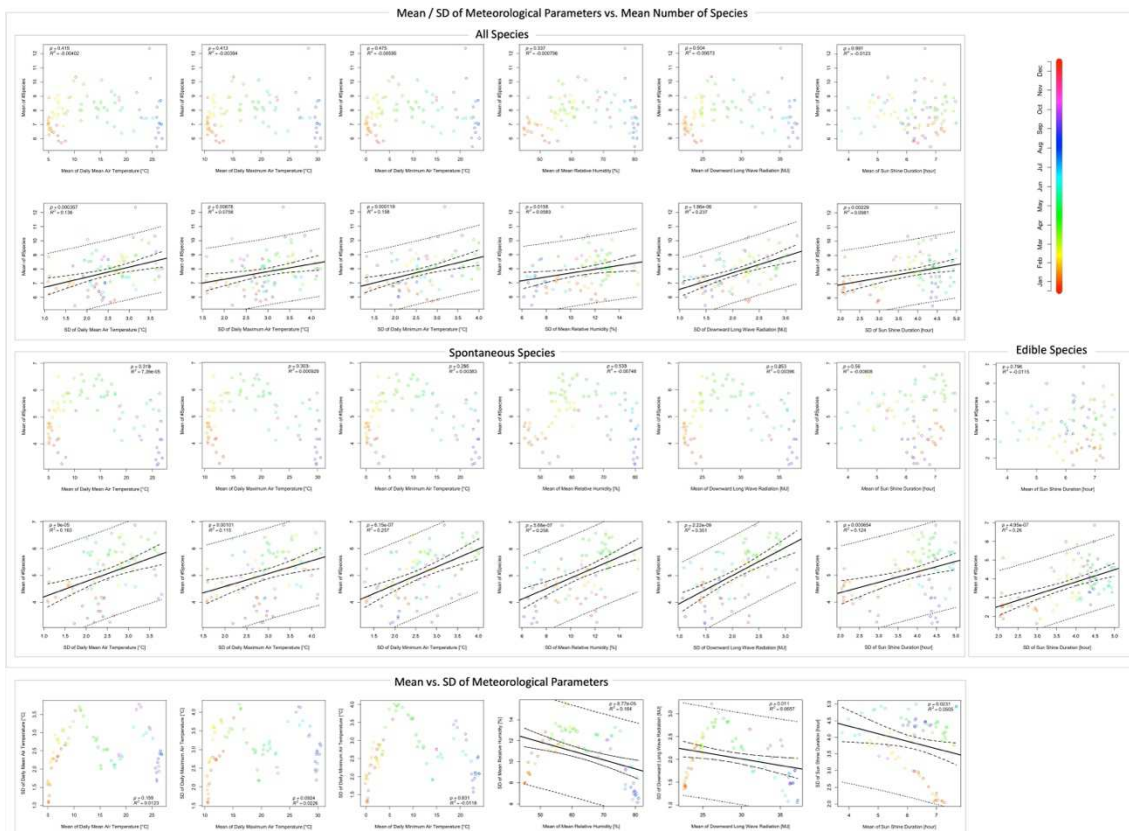
The optimum production range in conventional monoculture systems often ignores an important part of these parameters that may show the superiority of ecological optimum growth with mixed polyculture. For example, physiological optimization of the parameter *Env1* does not necessarily guarantee the superiority of monoculture production if another important parameter *Env2* remains marginal; in such case, the physiological optimum for *Env1* remains lower than the ecological optimum (e.g., monoculture millet production with and without association of other shrubs⁶¹). The results of the experiment in Burkina Faso imply that the conventional monoculture method was not totally optimized, and the changes in microclimate and soil environment affected by community dynamics dramatically improved the polyculture productivity in synecoculture.



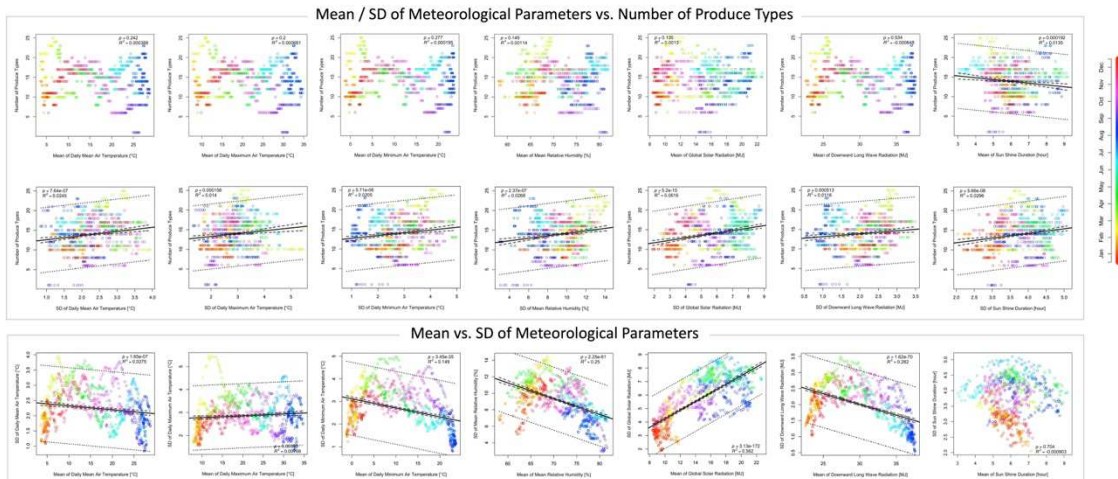
Extended Data Figure 1.

Left: Two-dimensional IMPEO. For simplicity, the case of a single crop without correlation between the mean environmental parameters is depicted.

939 **Right:** Two sections with fixed *Env2*.
 940 (a) Red line: Growth rate of a crop in isolation that defines the physiological
 941 optimum of *Env1* under the optimized *Env2*.
 942 (b) Red line: Example of actual monoculture productivity of the crop that controlled
 943 *Env1* but not *Env2*.
 944 (c) Blue line: Ecological optimum of the same crop with symbiotic gain in a
 945 mixed community with other plant species that did not affect *Env2*.
 946 (d) Blue line: Ecological optimum of the crop with symbiotic gain in a mixed
 947 community with other plant species, which ameliorated the *Env2* condition such as
 948 by changing microclimate and soil quality.
 949

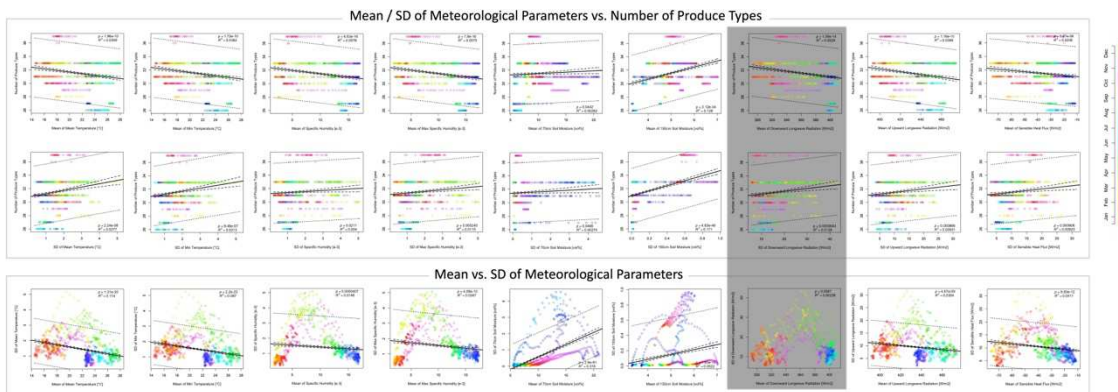


950 **Extended Data Figure 2. Mean species diversity in daily observed sections vs.**
 951 **monthly meteorological mean and variance during the second year of**
 952 **synecoculture introduction in the temperate zone (field A).** This is the complete
 953 data on which Fig 3 (b) in the main text is based. Results for six out of eight
 954 parameters that showed statistically significant positive correlations between species
 955 diversity and meteorological variance (standard deviation), and not the mean values,
 956 are shown according to the classification of plant species. No significant positive
 957 correlation was observed between the mean and standard deviation of each
 958 meteorological parameter. Black solid line: linear regression with less than 5%
 959 significance; dashed line: linear regression with 95% confidence; dotted line: linear
 960 regression with prediction intervals.
 961
 962



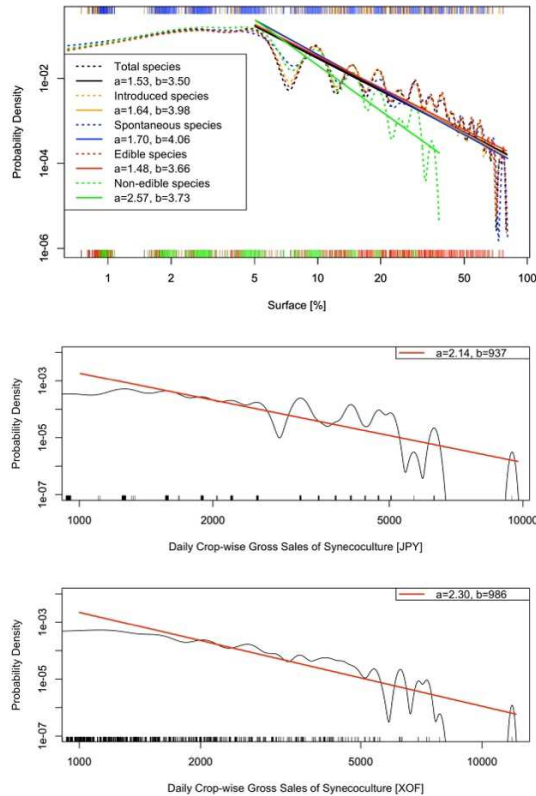
963
964
965
966
967
968
969
970
971
972
973
974
975

Extended Data Figure 3. Product diversity vs. meteorological mean and variance of synecoculture commercial production in the temperate zone (field B). This is the complete data on which Fig 4 (c) in the main text is based. Results of seven out of eight parameters that showed statistically significant positive correlations between the product diversity versus meteorological variance (standard deviation), and not the mean values, are shown. Although significant positive and negative correlations exist between the mean and standard deviation of the meteorological parameters, only the standard deviation showed significant positive correlations with the diversity of products. Black solid line: linear regression with less than 5% significance; dashed line: linear regression with 95% confidence; dotted line: linear regression with prediction intervals.



976
977
978
979
980
981
982
983
984
985
986
987

Extended Data Figure 4. Product diversity vs. meteorological mean and variance of synecoculture commercial production in the semi-arid tropical zone (field C). This is the complete data on which Fig 5 (c) in the main text is based. Results of nine out of 19 parameters that showed statistically significant positive correlations between the product diversity and meteorological variance (standard deviation) are shown. Only the standard deviation of downward longwave radiation exclusively correlated with product diversity (shaded in grey), while the other correlations can be alternatively explained as combinations of the correlations between the mean value of a meteorological parameter and product diversity and the correlation between the mean value and standard deviation of a meteorological parameter.



988
 989
 990
 991
 992
 993
 994
 995
 996
 997
 998
 999
 1000
 1001
 1002
 1003
 1004
 1005
 1006
 1007
 1008

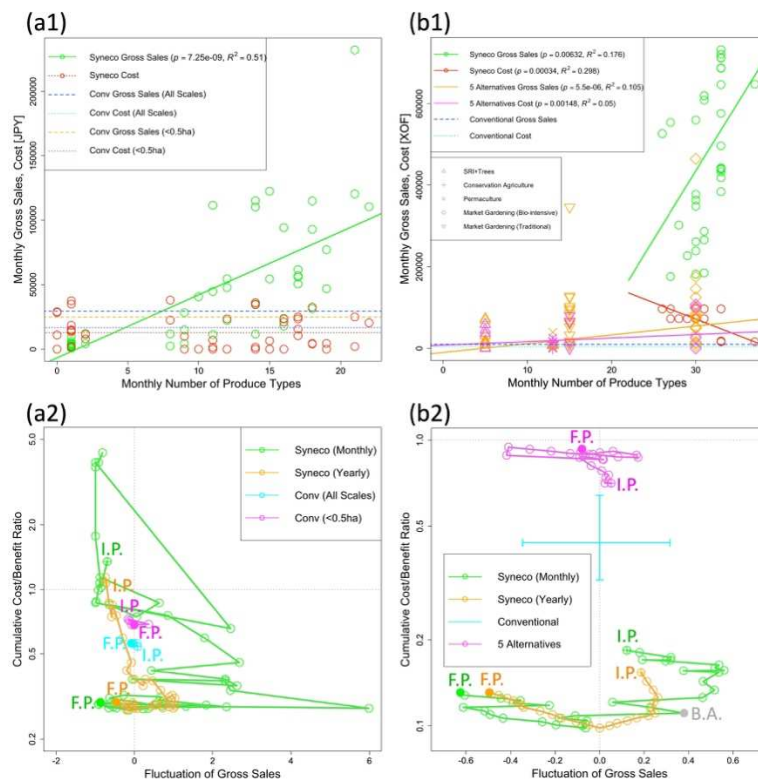
Extended Data Figure 5. Pareto distribution fitting of the species- and section-wise surface of field A and the crop-wise productivity of fields B and C.

The fitted parameters a and b of the Pareto distribution are shown in the legends. Note that the estimated values of b are inferior to the minimum of the x-axis ranges used for fitting, and the values $a > 1$ correspond to a Pareto distribution with finite mean value³⁰. The data are rug-plotted with the same color as the fitting on the bottom and top horizontal axes.

Top: Probability density of species-wise surface percentage data for 80 2-sq.m sections in the field A (dotted lines with colors according to the classification of plant species in the legend) [Supplementary Data 1]. The 2-sq.m section corresponds to the human scale for manual harvests in the other production experiments (middle and bottom). Double-logarithmic fitting with a Pareto distribution is plotted as solid lines with the same color.

Middle: Probability density of crop-wise daily sales data of the delivery box from the field B (black solid line) [Supplementary Data 2]. Double-logarithmic fitting with a Pareto distribution is plotted as a red solid line.

Bottom: Probability density of the crop-wise daily sales data of the field C (black solid line) [Supplementary Data 5]. Double-logarithmic fitting with a Pareto distribution is plotted as a red solid line.



1009
 1010
 1011
 1012
 1013
 1014
 1015
 1016
 1017
 1018
 1019
 1020
 1021
 1022
 1023
 1024
 1025
 1026
 1027
 1028
 1029
 1030
 1031
 1032
 1033
 1034
 1035
 1036

Extended Data Figure 6. Cost-benefit analysis of fields B and C.

(a1) Monthly aggregated number of synecoculture produce types sold from the field B (1,000 sq.m) plotted with respect to the monthly gross sales (green circles) [Supplementary Data 2] [Supplementary Data 3] and cost (red circles) in JPY [Supplementary Data 4]. The monthly number of produce types is the product diversity measured by the different number of crops listed in Fig 4 (b) and two additional kinds of products (seeds and seedlings, vegetables and fruits) sold on-site. Significant positive correlations between the gross sales and number of produce types are shown by the green solid line. No significant correlation was observed for cost versus produce types number. Monthly averaged gross sales and cost of conventional market gardening on 1,000-sq.m average in Japan⁵⁶ are plotted as comparative thresholds with the dashed blue line for gross sales of production for all scales, the dotted cyan line for the cost of production for all scales, the dashed orange line for the gross sales for farms less than 0.5 ha, and the dotted magenta line for the cost of production for farms less than 0.5 ha.

(a2) Fluctuation of gross sales (x-axis) versus cumulative cost divided by benefit ratio (y-axis) of the synecoculture production at the field B on a monthly scale (green circles connected with solid lines in monthly time series) and on a yearly scale (orange circles connected with solid lines in monthly time series). The productivity of yearly scale conventional market farming that covers the experimented period 2010-2014 is depicted as cyan circles connected by solid lines for production on all scales and as magenta circles connected by solid lines for small-scale (<0.5ha) production. Fluctuation of gross sales refers to the monthly gross sales minus the median of positive (non-zero) monthly gross sales for the green circles (synecoculture), the 12-month gross sales minus the median of all 12-month intervals' gross sales for the orange circles (synecoculture), and the yearly gross sales minus the mean of five years 2010-2014 for the cyan and magenta circles (conventional methods), all these are

1037 regularized with median (synecoculture) and mean value (conventional method). For
1038 each trajectory, the initial point (I.P.) and final point (F.P.) are depicted with a cross-
1039 marked circle and a filled circle, respectively.

1040 **(b1)** Monthly aggregated number of synecoculture produce types sold from the field C
1041 (500 sq.m) plotted with respect to the monthly gross sales (green circles)
1042 [Supplementary Data 5] and cost (red circles) in XOF [Supplementary Data 7]. Data of
1043 five alternative farming methods [Supplementary Data 6] are also plotted with
1044 different shapes (see the grey shapes in the legend). Significant positive correlations
1045 are depicted with solid lines, which are between the gross sales and produce types
1046 number of synecoculture (green solid line) and of the five alternative methods in total
1047 (orange solid line), and between the cost and produce types number of the five
1048 alternative methods in total (magenta solid line). A significant negative correlation is
1049 observed between the cost versus produce types number of synecoculture (red solid
1050 line). Monthly averaged gross sales and cost of conventional market gardening on 500-
1051 sq.m average in Burkina Faso⁵⁹ are plotted as comparative thresholds with the dashed
1052 blue line for the gross sales and with the dotted cyan line for introduction and water
1053 costs (see Methods).

1054 **(b2)** Fluctuation of gross sales (x-axis) versus cumulative cost divided by benefit ratio
1055 (Y-axis) of the synecoculture production at the field C on a monthly scale (green
1056 circles connected by green solid lines as a monthly time series) and on a yearly scale
1057 (orange circles connected by orange solid lines in a monthly time series). The average
1058 productivity of the five alternative farming methods [Supplementary Data 6] is also
1059 plotted on a yearly scale (magenta circles connected by solid lines in a monthly time
1060 series). Fluctuation of gross sales of synecoculture (green and orange circles) conforms
1061 to (a2), while that of the average of the five alternative methods (magenta circles)
1062 refers to the 12-month gross sales minus the median of all 12 month intervals' gross
1063 sales and is regularized with the median. The cyan lines with end bars represent the
1064 variable ranges of the gross sales (x-axis) and cumulative cost divided by benefit ratio
1065 (y-axis) for the 25th and 75th percentiles of conventional productivity (their intersection
1066 corresponds to the median value) based on the ten major crops in Burkina Faso (see
1067 Methods)⁵⁹.

1068 For each trajectory, the initial point (I.P.) and final point (F.P.) are depicted as in (a2).
1069 The event of a bandit attack (B.A.) in November 2016 near the field C is marked as a
1070 circle filled in grey; this event triggered a steep decline in the cost/benefit ratio by
1071 exacerbating the local security situation and causing loss of market access⁵⁸.
1072

1073 **References**

- 1074 61. Bogie, N. A. et al. Hydraulic redistribution by native sahelian shrubs -
1075 bioirrigation to resist in-season drought. *Front. Environ. Sci.* **6**, 98 (2018).
1076
1077
1078
1079
1080
1081